Journal of Photochemistry and Photobiology A: Chemistry 199 (2008) 211–223

Contents lists available at ScienceDirect

Journal of Photochemistry and Photobiology A: Chemistry

journal homepage: www.elsevier.com/locate/jphotochem

A theoretical study of the perfluoro-diarylethenes electronic spectra

François Maurel[a], Aurélie Perrier[a], Eric A. Perpète[b,1], Denis Jacquemin[b,*,1]

[a] *Laboratoire Interfaces, Traitements, Organisation et Dynamique des Systèmes (ITODYS), CNRS UMR7086, Université Paris 7-Denis Diderot, 1, rue Guy de la Brosse, 75005 Paris, France*

[b] *Laboratoire de Chimie Théorique Appliquée, Groupe de Chimie Physique Théorique et Structurale, Facultés Universitaires Notre-Dame de la Paix, rue de Bruxelles 61, B-5000 Namur, Belgium*

ARTICLE INFO

Article history:
Received 14 April 2008
Received in revised form 15 May 2008
Accepted 19 May 2008
Available online 27 May 2008

Keywords:
Diarylethenes
Photochromism
Density-functional theory
Colour
Electronic spectra

ABSTRACT

Using a combination of the time-dependent density functional theory and the polarizable continuum model, we have investigated the visible spectra of 129 closed-ring perfluorocyclopentene diarylethenes, solvated in various environments (185 cases). The theoretical simulations are able to reproduce the major experimental trends, especially the auxochromic shifts though solvatochromic effects in protic media are not correctly modelled. A quantitative agreement, that is mean absolute deviations limited to 13 nm or 0.05 eV, is reached with a simple linear regression. The topology of the frontier orbitals qualitatively support the role played by side groups, heteroatoms, as well as isomerism in the absorption phenomenon. Within similar structures, the bond length alternation in the central part of the photochrom can be related to the longest wavelength of maximal absorption (λ_{max}). In addition, a correlation between the central bond length and the thermal stability of the closed-ring form is unravelled.

1. Introduction

Initially proposed by the groups of Irie and Lehn [1–5], diarylethene (DA) derivatives are one of the most useful classes of photochromic molecules. Indeed, DA possess two thermally stable forms (either closed-ring or open-ring) that can be converted from one to the other by irradiation at well-separated wavelengths. Not only the direct and reverse conversions can be achieved a huge number of times but they also both present large quantum yields and short response times. The two forms have very different properties, with for instance, a colourless open-ring form, and a coloured closed-ring form. Consequently, DA are ideal candidates for building photo-switches or optical storages, and their synthesis (and properties) have been reviewed by several authors since 2000 [6–11]. One usually classifies DA derivatives according to their bridge unit, i.e. the group linking the two parts in the open-form. DA with cyano [1,12], maleic [1,13], perfluorocycloalkanes [14], maleimide [15], oxazole [16], thiazole [16], imidazole [16], cyclopentene [17,18], dihydrothiophene [19], furanone [20] and dihydropyrrole [21,22] linkages have been designed. However, since the investigation of Hanazawa *et al.* it is clear that the use of perfluorocyclopentene-DA has many practical advantages [14], and most today's DA rely on this bridge. These perfluoro-DA offer very versatile applications that are not limited to single-molecule photochromism in solvent medium. Let us highlight three more complex processes: (1) DA can be used as magnetic switches as the spin–spin couplings between the two side rings are greatly influenced by a ring closure [23]; (2) with adequate side groups, one can combine photon- and electron-triggered cyclisation, and create electrochemically controlled switches [24]; (3) perfluoro-DA also have the ability to perform reversible crystal shape modifications [25], that take place at microsecond scale, i.e. much faster than in liquid crystals. Such developments pave the way towards new promising applications such as photon-triggered nano-slings, photomagnetic devices or electrochemical remote controls. In this work, our first goal is to obtain an *ab* initio theoretical procedure able to predict the colour of DA molecules. Designing such scheme subsequently allows a rapid screening of this important property of the photo-switches. We also aim at establishing structure–property relationships for DA, in order to guide the design of new photochroms. Up to now, considerable theoretical efforts have been devoted to the simulation of the photo-closure of DA, for which calculations have been performed using an extended panel of models, and we refer the reader to Refs. [17,26–34] for selected examples. On the contrary, fewer works have been devoted to the computation of the absorption spectra (see below).

Here, our main theoretical tool is the time-dependent density functional theory (TD-DFT) that is now the most popular *ab* initio

* Corresponding author. Tel.: +32 81 724557; fax: +32 81 724567.
E-mail address: denis.jacquemin@fundp.ac.be (D. Jacquemin).
URL: http://www.perso.fundp.ac.be/ jacquemd (D. Jacquemin).

[1] Research Associate of the Belgian National Fund for Scientific Research.

1010-6030/$ – see front matter © 2008 Elsevier B.V. All rights reserved.
doi:10.1016/j.jphotochem.2008.05.018

technique for evaluating electron transition energies of medium-sized systems. A great advantage of TD-DFT is that solvent effects can be straightforwardly included for both absorption [35] and emission properties [36,37]. When conventional hybrid functionals are used TD-DFT is generally a robust approach that gives accurate estimates for organic dyes having a chromophoric unit centered on a few atoms [38–40], whereas its main deficiency is the significant underestimation of the transition energies involving charge-transfer states [41]. This problem can be solved by using refined *ab* initio wavefunction approaches such as EOM-CC, SAC-CI or CAS-PT2, but all are computationally non-tractable to study large sets of molecules. On the contrary, semi-empirical schemes could be valuable tools to gain chemical insights, and might reproduce the main experimental trends, but definitively lack of consistency. For DA, it has been shown that, on the one hand, TD-DFT and SAC-CI results are in good agreement with each other for neutral structures [42], while, on the other hand, the ZINDO//AM1 (property calculation method//geometry optimization scheme is much less accurate than TD-DFT for predicting auxochromic displacements [43]. These previous studies obviously justify the use of TD-DFT in the present investigation. While several gas-phase and small basis sets TD-DFT computations of the absorption spectra of DA are available in the literature [34,44–53], most of them remain focussed on a few (3–10) compounds. In this work, we investigate a very extended set of molecules by using the computational procedure successfully applied to other classes of DA derivatives [43,54–56]. We have recently demonstrated that after linear corrections, our methodology based on the PBE0 functional provides very consis-

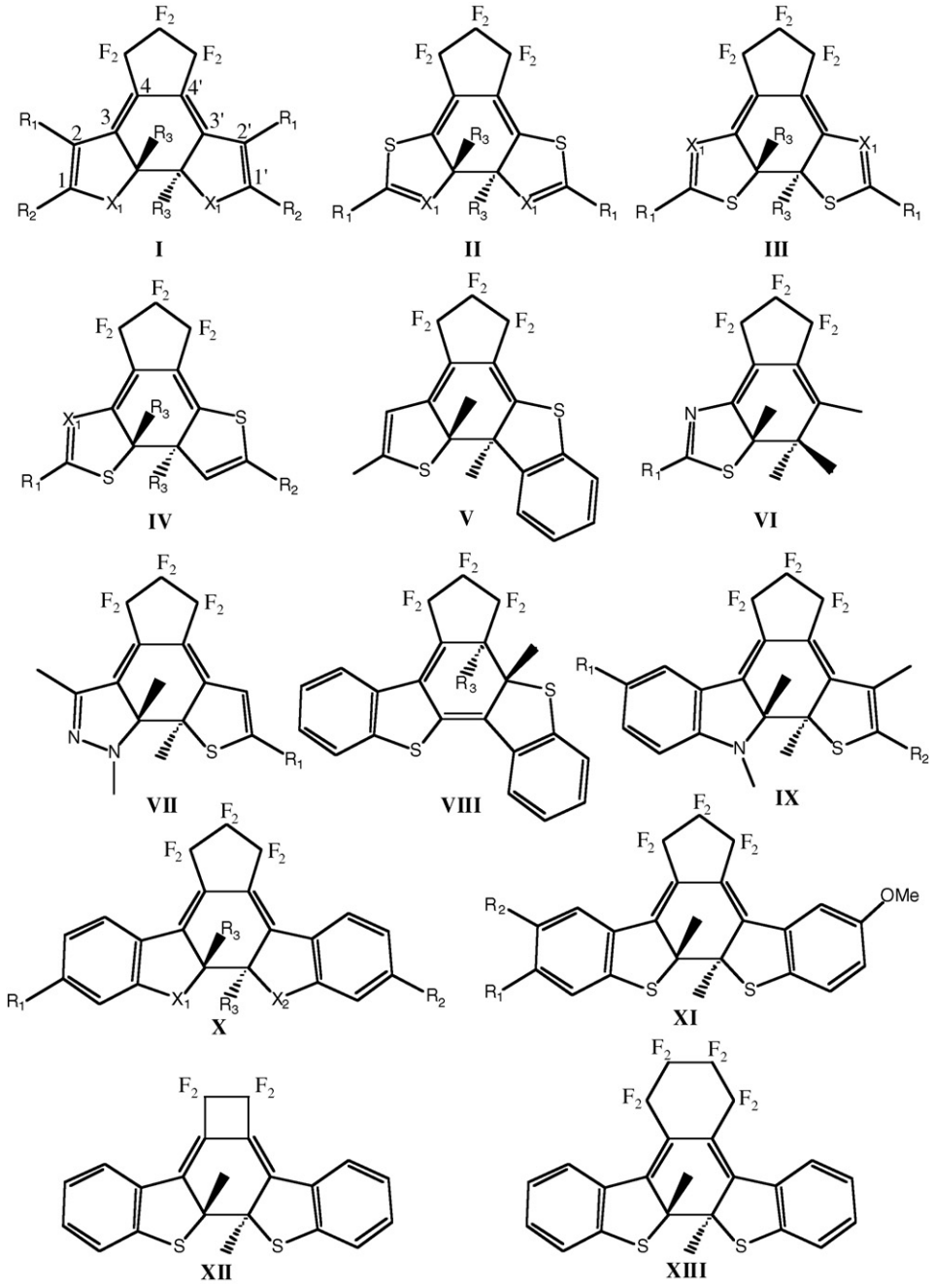

Fig. 1. Sketch of the investigated diarylethenes.

tent wavelengths of maximal absorption for cyclopentene-DA [56]. To limit such corrections [57], one could lean towards a range-separated hybrid (namely CAM-B3LYP) [58] but this functional is not yet available in commercial packages. This paper is organized as follows: in Section 2 we describe our computational procedure; in Section 3.1 we compare the computed wavelengths with available experimental data; in Section 3.2 we establish structure–property relationships, and in Section 4 we provide a brief summary.

2. Methodology

We have used the Gaussian03 [59] package of programs to perform the geometry optimizations, vibrational analysis and excited state evaluations for the full set of DA derivatives drawn in Fig. 1. All calculations have been performed with the hybrid PBE0 functional (sometimes named PBEh or PBE1PBE) [60,61], that was designed on purely theoretical considerations [60–62]. PBE0 has indeed been found successful for cyano, maleic and cyclopentene-based photochroms [43,54,56], as well as for numerous classes of organic dyes [63–67,40]. The bulk solvent effects are evaluated by means of the polarizable continuum model (PCM) [68], as we demonstrated that modelling the medium effects is a prerequisite to valuable comparisons with experiments [35,63–65,69]. Several solvents have been used: cyclohexane (CH), hexane (Hex) [70], 3-methyl-pentane (MP) [71], benzene (Benz), toluene (Tol), chloroform (CHL), dichloromethane (DCM), 1,2-dichloroethane (DCE), diethylether (DEE) [72], ethyl acetate (EA) [73], tetrahydrofuran (THF), ethanol (EtOH) or acetonitrile (ACN). The cavity lodging the dye has been constructed with the UA0 (United Atom Topological Model, optimized using UFF force field) radii, but during some geometry optimizations for which the UAKS (United Atom Topological Model, optimized using the PBE0/6-31G(d) level of theory) radii were necessary to obtain converged ground-state structures [59,68].

For each system, the ground-state structure has been determined in condensed phase by a standard force-minimization process, and the vibrational spectrum has been systematically [74] computed at the same level of theory to check that all vibrational frequencies are real. These ground-state calculations have been performed with a triple-ζ polarized basis set, 6-311G(d,p), that is known to provide converged ground-state structural parameters for DA [43,54] as well as for most organic molecules [75–77]. For the iodine atom, the well-known LanL2DZ pseudopotential/basis set replaces 6-311G(d,p).

TD-DFT, within the non-equilibrium PCM approach, is then used to compute the low-lying excited states of DA. TD-DFT calculations rely on the 6-311+G(2d,p) basis set, as any further extension of the basis set does not alter the λ_{max} of DA [43,54], i.e. 6-311+G(2d,p) provides converged transition energies. Similarly to the optimization step, LanL2DZ pseudopotential/basis set replaces 6-311+G(2d,p) for the iodine atom.

3. Results

3.1. Comparisons with experimental data

Experimental and theoretical λ_{max} are reported in Table 1 for the perfluoro-DA derivatives. This represents an extended set of 129 photochroms, several in various solvents, for a total of 185 cases. To the very best of our knowledge that is the largest set of DA data ever treated with TD-DFT. In fact, this table includes all the perfluoro derivatives for which experimental data are available, provided the molecular size allows a feasible calculation (3 weeks cpu-time limit on 2.8 GHz Xeon PC). Note that several measurements have been carried out at the photostationary state. In such case, the closed-ring λ_{max} are deduced from variations induced by irradiation. For some compounds, several experiments are available and it turns out that, besides a likely misprint (526 nm instead of 562 nm in Ref. [30]) and a clear inconsistency (505 nm versus 530 nm for the SO_2-**X**, by the same authors), substantial discrepancies (up to 10 nm) can be detected. This illustrates that experimental reference values can never be considered as error-free.

It turns out that all molecules belong to the C_1 point group, even for the compounds with a symmetric substitution pattern. The only exceptions are DA **XII** and **XIII**, that are found to be C_2. This is consistent with the work of Yokojima *et al.* [42], who concluded that the five-member bridges do break the axial symmetry. By imposing a C_2 symmetry for the energy minimization process of **I** with X =S, $R_{1,3}$=Me, and R_2=*p*-Pyr (benzene media), one obtains an unstable DA geometry with one imaginary frequency of 39*i* cm^{-1} corresponding to the out-of-plane deformation of the top CF_2 group (see Fig. 1). The total Gibbs free energy difference with respect to the stable C_1 form is relatively small: +3.13 kcal/mol. In the same way, for a typical **X** ($X_{1,2}$=S, $R_{1,2}$=H, R_3=Me in hexane), the C_2 form is less stable than its C_1 counterpart by 3.0 kcal/mol only. On the contrary, the discrepancies between the electronic absorption spectra computed for the C_2 and C_1 structures are significant. Indeed, the C_2 λ_{max} is too large by 19 nm (673 nm instead of 654 nm) in the first case, and by 17 nm (567 nm instead of 550 nm) in the second. This contrasts with the model system found in Ref. [42], for which in the neutral state, the excited state energies were completely similar for C_1 and C_2 structures. Consequently, all calculations presented in this work have been performed within the correct C_1 point group. For **I** with X = S and two CH =$C(CN)_2$ moieties, we optimized two conformers with different orientations of the side groups, the left structure of Fig. 2 being more stable by 2.4 kcal/mol (Gibbs energy at the PCM-PBE0/6-311G(d,p) level). Note that their λ_{max} also differ: 898 nm for the right conformer, 871 nm for the left one. For **I** with two CHO side groups, we have found that the structure with the oxygen alongside the sulphur atoms is more stable (by 4.9 kcal/mol) than the conformer with the reverse symmetry (see Fig. 2). The system with the two carbonyl differently oriented being, as expected, intermediate (2.0 kcal/mol). These two latter conclusions are completely consistent with the findings of Ref. [50] for cyclopentene systems. For the DA with thiophene rings on the reactive carbon atoms [78], we have found two minima displayed in Fig. 2. For the photochrom with no side groups, the Gibbs energy difference (ΔG) is limited to 0.7 kcal/mol in favour of the system with the most distant sulphur atoms. When adding sulphur groups at R_2, the same energetic ranking pertains but with a ΔG down to 0.08 kcal/mol, i.e. smaller than the (room) thermal energy. As the λ_{max} related to the two conformers are significantly different (670 nm for the most stable and 690 nm for the least stable), we have used a Boltzmann-averaged value (679 nm) below.

Before comparing raw λ_{max}, it is important to assess the chemical reliability of the model, i.e. is TD-DFT adequate (or not) to provide correct chemical insights for perfluoro-DA? Table 1 shows that most auxochromic effects are correctly foreseen by theory, though their amplitudes tend to be overestimated for the strongly electro-active groups that provokes significant charge-transfer upon photon absorption. With standard hybrid DFT functional, such cases are indeed problematic to cope with [41]. A typical theoretical success is met for the **I** series. Indeed, in hexane, replacing the side R_2=methyl by R_2=H, R_2=Cl and R_2=F (keeping X_1=S, R_1=H and R_3=Me) induces respective experimental displacements of +6, +3 and −39 nm of the λ_{max}, that are nicely reproduced by theory: +13, +4 and −39 nm. The same TD-DFT reliability holds when using bulkier substituents such as 1,3-dithiolpentane, phenyl or *p*-F-Ph instead of alkyl at R_2 position, with respective experimental

Table 1
λ_{max} (in nm) for the diarylethene derivatives of Fig. 1

	Substitution					Solvent	λ_{max}		
	X_1	X_2	R_1	R_2	R_3		Theo.	Exp.	Ref
I	CH=CH	–	H	*t*-Bu	Me	Hex	602	518	[94]
	CH=CMe	–	Me	H	Me	Hex	609	527	[94]
	S	–	Me	H	Me	Hex	558	527, 534, 534	[95,4,96]
	S	–	Me	Me	Me	Hex	548	525	[47]
	S	–	Cl	Me	Me	Hex	556	528	[47]
	S	–	F	Me	Me	Hex	560	530	[47]
	S	–	Me	CN	Me	Tol	651	588	[97]
	S	–	Me	*p*-CN-Thioph.	Me	Tol	708	630	[97]
	S	–	Me	Ph	Me	Hex	606	562, (526), 562	[4,30,98]
	S	–	Me	Ph	*i*-Pr	Hex	580	586	[30]
	S	–	Me	*p*-OMe-Ph	Me	Hex	609	597	[4]
	S	–	Me	*p*-NEt_2-Ph	Me	Hex	628	597	[4]
	S	–	Me	*p*-CN-Ph	Me	Hex	634	570	[4]
	NMe	–	H	CN	Me	EA	681	630	[99,100]
	NMe	–	H	$CONH_2$	Me	EA	620	631	[100]
	NMe	–	H	CO_2Me	Me	EA	707	660	[100]
	NMe	–	H	CO_2H	Me	EA	712	644	[100]
	NMe	–	H	Ph	Me	EA	627	618	[100]
	NMe	–	H	Thioph.	Me	EA	658	656	[100]
	NMe	–	H	C≡CH	Me	EA	662	636	[100]
	S	–	H	H	H	Hex	497	469	[47]
	S	–	H	H	F	Hex	605	539	[47]
	S	–	H	H	Me	Hex	540	509	[47]
	S	–	H	H	Me	DCM	544	520	[78]
	S	–	H	H	Thioph.	DCM	598	545	[78]
	S	–	H	Me	Me	Hex	527	505, 503	[45,47]
	S	–	H	Me	Me	CH	529	505	[101]
	S	–	H	Cl	Me	Hex	531	501, 506	[102,18,47]
	S	–	H	Cl	Me	ACN	535	504, 501	[103,50]
	S	–	H	F	Me	Hex	488	464	[47]
	S	–	H	I	Me	ACN	544	514	[50]
	S	–	H	*p*-Pyr.	Me	Benz	654	592, 592	[3,5]
	S	–	H	*p*-Pyr.	Me	DCM	655	592, 592	[3,5]
	S	–	H	CHO	Me	Benz	702	624, 624	[3,5]
	S	–	H	CHO	Me	Tol	703	625	[104]
	S	–	H	CHO	Me	DCM	704	624, 619	[3,5]
	S	–	H	CHO	Me	ACN	700	614, 606	[103,50]
	S	–	H	COOH	Me	ACN	620	586	[105]
	S	–	H	COMe	Me	Tol	590	625	[106]
	S	–	H	CH_2OH	Me	Tol	538	515, 515	[106,104]
	S	–	H	SEt	Et	Tol	573	540, 540	[106,104]
	S	–	H	SEt	Et	EtOH	573	564, 564	[107,108]
	S	–	Br	SEt	Et	EtOH	643	592	[108]
	S	–	COOH	SEt	Et	EtOH	575	568	[108]
	S	–	H	$CH=C(CN)_2$	Me	Benz	871	729, 727	[3,5]
	S	–	H	$CH=C(CN)_2$	Me	CHL	875	724	[109]
	S	–	H	CH=N-NMe_2	Me	CHL	650	622	[110]
	S	–	H	*p*-TMS-Thioph.	Me	DCE	667	620	[111]
	S	–	H	TMS	Me	ACN	574	554	[50]
	S	–	H	TMS	OMe	Hex	654	599	[112]
	S	–	H	1,3-dithiol-pentane	Me	Hex	560	528	[113]
	S	–	H	1,3-dithiol-pentane	Me	CHL	565	528	[113]
	S	–	H	1,3-dithiol-pentane	Me	DEE	562	532	[113]
	S	–	H	1,3-dithiol-pentane	Me	ACN	565	534	[113]
	S	–	H	1,3-dioxo-pentane	Et	Hex	572	542	[114]
	S	–	H	Thioph.	Me	DCM	654	625	[78]
	S	–	H	Thioph.	Me	ACN	651	605	[115]
	S	–	H	*p*-Me-Thioph.	Me	ACN	655	612	[115]
	S	–	H	Thioph.	Thioph.	DCM	679	632	[78]
	S	–	H	Ph	Me	Hex	630	575, 575, 585, 575	[116,89,102,117]
	S	–	H	Ph	Me	CH	632	590	[118]
	S	–	H	Ph	Me	CHL	632	585	[110]
	S	–	H	Ph	Me	ACN	630	588, 588	[119,103]
	S	–	H	Ph	*i*-Pr	Hex	682	600	[120]
	S	–	H	Ph	OMe	Hex	635	625, 625	[121,116]
	S	–	H	Ph	CN	Hex	596	545	[116]
	S	–	H	Ph	CH_2OMe	Hex	650	580	[116]
	S	–	H	Ph	OEt	Hex	639	625	[121]
	S	–	H	*o*-CHO-Ph	Me	CH	575	553	[122]
	S	–	H	*o*-CHO-Ph	Me	EtOH	579	549	[122]
	S	–	H	*m*-CHO-Ph	Me	CH	639	585	[122]
	S	–	H	*m*-CHO-Ph	Me	EA	639	588	[123]
	S	–	H	*m*-CHO-Ph	Me	EtOH	638	581	[122]

Table 1 (*Continued*)

	Substitution					Solvent	λ_{max}		
	X_1	X_2	R_1	R_2	R_3		Theo.	Exp.	Ref
	S	–	H	*p*-CHO-Ph	Me	CH	692	605	[122]
	S	–	H	*p*-CHO-Ph	Me	EtOH	695	601	[122]
	S	–	H	*o*-COOH-Ph	Me	CH	570	567	[122]
	S	–	H	*o*-COOH-Ph	Me	EtOH	594	546	[122]
	S	–	H	*m*-COOH-Ph	Me	CH	638	584	[122]
	S	–	H	*m*-COOH-Ph	Me	EtOH	634	580	[122]
	S	–	H	*p*-COOH-Ph	Me	CH	673	598	[122]
	S	–	H	*p*-COOH-Ph	Me	EtOH	671	600	[122]
	S	–	H	*p*-CN-Ph	Me	Hex	675	592	[102]
	S	–	H	*p*-CN-Ph	Me	CHL	680	606	[110]
	S	–	H	*p*-CN-Ph	Me	ACN	678	586	[103]
	S	–	H	*o*-F-Ph	Me	Hex	635	577	[124]
	S	–	H	*m*-F-Ph	Me	Hex	635	579, 579	[124,125]
	S	–	H	*m*-CF_3-Ph	Me	Hex	635	566	[126]
	S	–	H	*m*-CF_3-Ph	Me	Tol	639	580	[126]
	S	–	H	*m*-CF_3-Ph	Me	DEE	634	572	[126]
	S	–	H	*m*-CF_3-Ph	Me	THF	635	578	[126]
	S	–	H	*m*-CF_3-Ph	Me	EA	634	578	[126]
	S	–	H	*m*-CF_3-Ph	Me	DCM	636	580	[126]
	S	–	H	*m*-CF_3-Ph	Me	EtOH	634	574	[126]
	S	–	H	*m*-CF_3-Ph	Me	ACN	633	576	[126]
	S	–	H	*p*-F-Ph	Me	Hex	626	570, 570	[127,124]
	S	–	H	*p*-Me-Ph	Me	Hex	632	580	[89]
	S	–	H	*p*-OEt-Ph	Me	Hex	634	584	[127]
	S	–	H	*p*-OH-Ph	Me	ACN	630	590, 590, 590	[128–130]
	S	–	H	*p*-OMe-Ph	Me	Hex	633	582, 587	[131,102]
	S	–	H	*p*-OMe-Ph	Me	CHL	637	592	[110]
	S	–	H	*p*-OMe-Ph	Me	ACN	634	593, 593	[119,103]
	S	–	H	*p*-NMe_2-Ph	Me	Hex	656	602	[127]
	S	–	H	*p*-NMe_2-Ph	Me	ACN	663	606	[132]
	S	–	H	*p*-tBu-Ph	Me	Hex	634	580	[89]
II	N	–	Ph	–	CF_3	DCM	454	420	[133]
	N	–	Me	–	Me	Hex	407	391	[134]
	N	–	Ph	–	Me	Hex	426	406	[134]
	N	–	*p*-OMe-Ph	–	Me	Hex	423	402	[134]
	CH	–	Me	–	Me	Hex	452	425, 425	[96,135]
	CH	–	H	–	Me	MP	462	432	[136]
	N	–	*o*-Pyr.	–	Me	ACN	431	414	[46]
III	N	–	Me	–	OEt	Hex	499	474	[134]
	N	–	Ph	–	Me	Hex	554	525	[134]
	N	–	Ph	–	Me	Tol	556	534	[137]
	N	–	Ph	–	OMe	Tol	542	555	[137]
	N	–	*o*-Pyr.	–	Me	ACN	558	545	[46]
IV	CMe	–	H	Me	Me	Hex	494	469	[96]
	CH	–	Me	Me	Me	Hex	487	469	[135]
	CH	–	Me	Ph	Me	Hex	497	468	[138]
	CH	–	*p*-OMe-Ph	*p*-OMe-Ph	Me	Hex	539	506	[138]
	CH	–	Me	*p*-OMe-Ph	Me	Hex	495	468	[138]
	N	–	Ph	H	Me	Tol	519	494	[139]
	N	–	Ph	H	OMe	Tol	540	525	[139]
V	–	–	–	–	–	Hex	477	466	[138]
VI	–	–	*p*-OMe-Ph	–	–	Tol	431	416	[139]
VII	–	–	*o*-OMe-Ph	–	–	Hex	604	573	[140]
	–	–	*m*-OMe-Ph	–	–	Hex	598	573	[140]
	–	–	*p*-OMe-Ph	–	–	Hex	598	573	[140]
III	–	–	–	–	Me	Hex	529	504	[141]
	–	–	–	–	OMe	Hex	534	510	[141]
IX	–	–	OMe	CN	–	Hex	688	665	[142]
X	CH_2	O	H	H	Me	Hex	466	435	[143]
	CH_2	S	H	H	Me	Hex	495	469	[143]
	CH=CH	CH=CH	H	H	Me	Hex	533	471	[144]
	NMe	S	H	H	Me	Hex	567	556	[145]
	O	O	H	H	Me	Hex	500	469, 469	[146,147]
	O	O	H	H	Me	EA	502	476	[146]
	O	O	H	H	Me	THF	503	479	[146]
	O	O	H	H	Me	EtOH	503	475	[146]
	O	O	H	H	Me	ACN	502	476	[146]
	O	O	H	H	*n*-Bu	Hex	503	489	[146]
	O	O	H	H	*n*-Bu	EA	506	495	[146]
	O	O	H	H	*n*-Bu	THF	506	498	[146]
	O	O	H	H	*n*-Bu	EtOH	506	495	[146]
	O	O	H	H	*n*-Bu	ACN	507	496	[146]
	O	S	H	H	Me	Hex	519	493	[147]
	O	S	H	H	Et	Hex	546	507	[147]

Table 1 (*Continued*)

	Substitution					Solvent	λ_{max}		
	X_1	X_2	R_1	R_2	R_3		Theo.	Exp.	Ref
	O	S	H	H	*n*-Pr	Hex	546	507	[147]
	O	S	H	H	*n*-Bu	Hex	547	508	[147]
	S	S	H	H	Me	Hex	550	517, 517, 517, 517, 517, 517	[148,145,116,146,143,147]
	S	S	H	H	Me	CH	551	517	[149]
	S	S	H	H	Me	Benz	552	526	[14]
	S	S	H	H	Me	CHL	553	534	[150]
	S	S	H	H	Me	EA	552	523, 523, 517, 522, 523, 523	[151,23,152,146,153,53]
	S	S	H	H	Me	THF	553	523	[146]
	S	S	H	H	Me	EtOH	553	521	[146]
	S	S	H	H	Me	ACN	553	521	[146]
	S	S	H	H	Et	Hex	559	536	[154]
	S	S	H	H	*i*-Pr	Hex	536	535, 535	[148,120]
	S	S	H	H	*n*-Pr	Hex	558	533	[154]
	S	S	H	H	*n*-Bu	Hex	559	535, 536	[146,154]
	S	S	H	H	*n*-Bu	EA	563	542	[146]
	S	S	H	H	*n*-Bu	THF	564	545	[146]
	S	S	H	H	*n*-Bu	EtOH	565	542	[146]
	S	S	H	H	*n*-Bu	ACN	565	544	[146]
	S	S	H	H	OMe	Hex	531	547	[116]
	S	S	H	H	CN	Hex	530	496	[116]
	S	S	H	H	CH_2OMe	Tol	565	520, 520	[106,104]
	S	S	Ph	Ph	Me	EA	577	543	[23]
	S	S	OMe	OMe	Me	CH	541	520	[149]
	S	S	COMe	H	Me	Tol	579	545	[106]
	S	S	COMe	COMe	Me	Tol	602	545	[106]
	S	S	CHO	H	Me	Tol	587	555	[104]
	S	S	CHO	CHO	Me	Tol	613	545	[104]
	S	S	NO_2	H	Me	CHL	608	552	[150]
	S	S	NO_2	NO_2	Me	Hex	619	545	[90]
	S	S	NO_2	NO_2	Me	CHL	632	559	[150]
	S	S	NO_2	NO_2	CH_2OMe	Tol	630	545, 545	[106,104]
	S	S	NO_2	DOThio	Me	CHL	647	587	[150]
	S	SO_2	H	H	Me	EA	526	(530), 505	[155,53]
	SO_2	SO_2	H	H	Me	EA	424	400, 398, 398	[156,155,53]
XI	–	–	H	OMe	–	CH	590	569	[149]
	–	–	OMe	H	–	CH	567	542	[149]
XII	–	–	–	–	–	Benz	551	532	[14]
XIII	–	–	–	–	–	Benz	541	510	[14]

All theoretical values are computed within the PCM-TD-PBE0/6-311+G(2d,p)//PCM-PBE0/6-311G(d,p) methodology. See text for more details.

(theoretical) $\Delta\lambda_{max}$ of +24 nm (+33 nm), +76 nm (+103 nm) and +66 nm (+99 nm). In cyclohexane, adding aldehyde groups at the *o*, *m* or *p* position(s) of the side phenyl rings of **I** leads to −37, −5 and +15 nm wavelength variations, that are less accurately estimated by theory to be -57, +6 and +60 nm. For **X**, trading both side hydrogens attached at R_1 and R_2 for Ph, OMe, CHO and NO_2 gives measured (calculated) λ_{max} changes of +23 nm (+25 nm), −3 nm (−10 nm), +19 nm (+61 nm) and +28 nm (+69 nm), respectively; i.e. theory overestimates the auxochromic effects for groups presenting a significant charge-transfer character. This nice overall performance parallels the cyclopentene-DA success collected in our previous investigation [56]. Variations of the position of the heteroatoms within the reactive five-member rings such as **I**→**IV**, **IV**→**II** and **X**→**III** induce experimental hypsochromic shifts of −36, −44 and −13 nm, correctly estimated by TD-DFT: −40, −35 and −21 nm, respectively. In the **X** series, one can straightforwardly evaluate the impact of the heteroatoms included in the five-member rings. Keeping the other parameters unchanged (as well as the medium), going from X_1/X_2=S/S to O/S, O/O, CH_2/O, CH_2/S, NMe/S, S/SO_2 and SO_2/SO_2 brings experimental (theoretical) λ_{max} shifts of −24 nm (−31 nm), −48 nm (−50 nm), −82 nm (−84 nm), −48 nm (−55 nm), +39 nm (+17 nm), −15 nm (−26 nm) and −121 nm (−128 nm), respectively. Similarly for **II** the replacement of the nitrogen atoms by CH moieties at X_1, provokes a bathochromic shift of +34 nm (+45 nm with TD-DFT). The impact of substitutions at the reactive carbon, that is modification of the R_3 groups (see Fig. 1), are generally correctly predicted. For instance, for **I** with X_1=S, R_1=H and R_2=Ph, going from methyl to cyano groups at R_3, leads to a hypsochromic displacement of −35 nm (−34 nm). Likewise, for **X** with X_1=S, X_2=S or O, and $R_{1,2}$=H, increasing the alkyl chain length at R_3 has a large impact for the first step (from Me to Et) but negligible spectral modifications are detected for further increments (from Et to *n*-Pr or *n*-Bu) in both theory and experiment. On the contrary, the spectral variations due to alkoxy and *i*-Pr groups are generally poorly estimated. For the OMe group, such problems were already reported for indigoïds [39], and were attributed to the various possible orientations of the methyl group. In short, PCM-TD-PBE0 correctly reproduces the main experimental trends, although some problems pertain, especially for alkoxy, aldehyde and nitro derivatives, as well as for alcoholic solutions.

For numerous DA, the absorption wavelengths have been determined in several apolar or polar environments. Both correct estimates and dramatic errors can be found in Table 1. In the first category, one notes *p*-NMe_2Ph-**I** and 1,3-dithiolpentane-**I** with respective experimental (theoretical) solvatochromic shifts of +4 nm (+7 nm) and +6 nm (+5 nm) when going from hexane to acetonitrile. The same accurate simulations holds for *p*-OMe_2Ph-**I** or NO_2-**X** that respectively undergo a +7 nm (+4 nm) and +14 nm (+13 nm) positive solvatochromism effects, when changing hexane to chloroform. In the second category, we have to point out *o*-COOH-Ph-**I**, with a large PCM estimate (+24 nm) suffering a sign error (exp = −21 nm) when replacing cyclohexane by ethanol. Such an experimental negative solvatochromic effect is unexpected

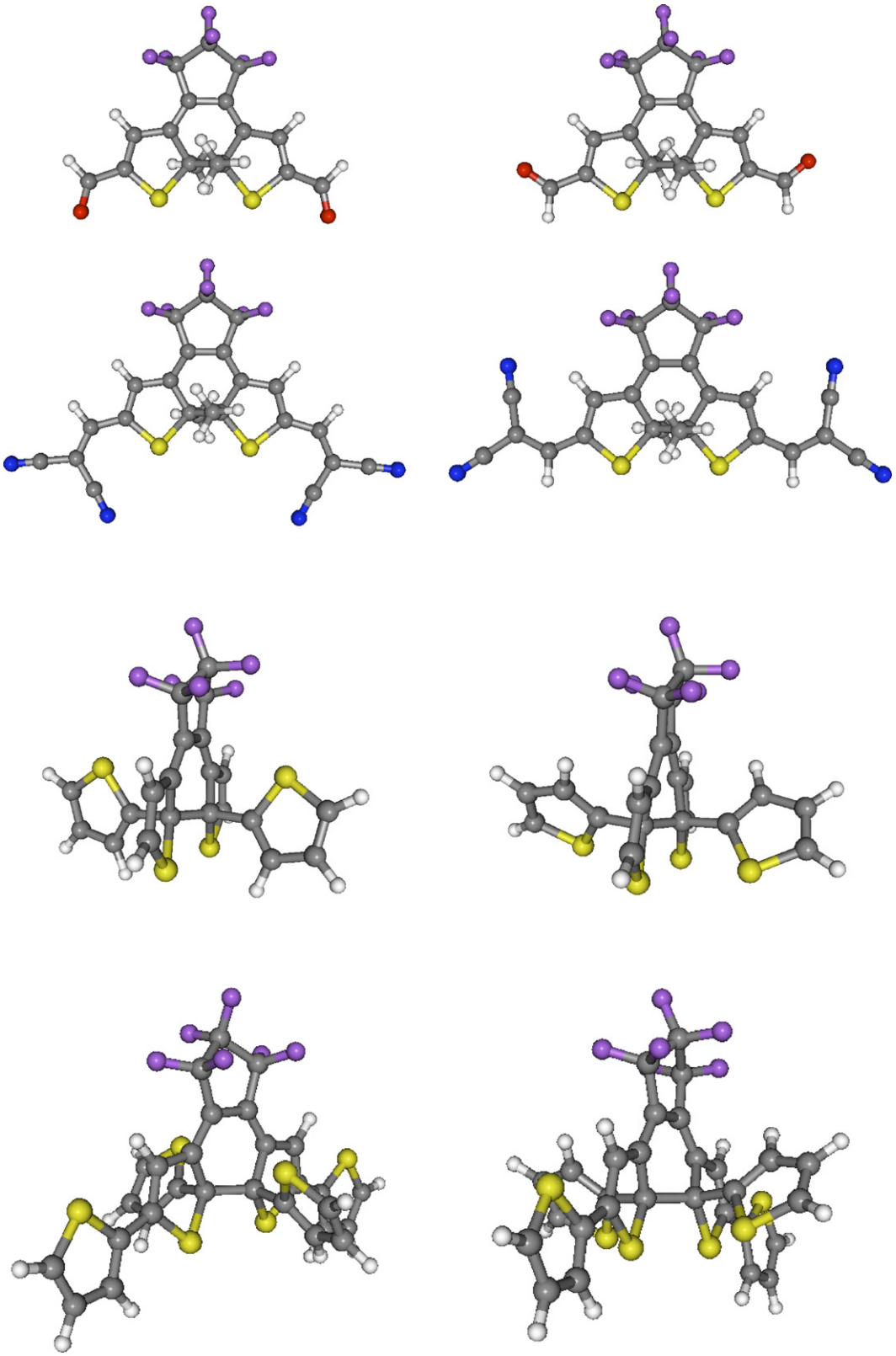

Fig. 2. Illustration of the conformers optimized for **I** with (from top to bottom) CHO side groups, CH =C(CN)$_2$ side groups, thiophene rings at R$_3$ and thiophene rings at both R$_2$ and R$_3$. For all compounds, the most stable structures are located on the left of the figure. See text for more details.

for a $\pi \rightarrow \pi^*$ transition, and therefore indicates the presence of solute–solvent hydrogen bonds, highly probable for acidic structures likes carboxylic groups. The ability of the PCM model to reproduce the solvatochromic effects is obviously limited by the lack of specific description of the solute–solvent interactions. Anyway, removing completely the environmental modelling from our theoretical approach would lead to significantly worse data, as demonstrated in our previous investigations [39].

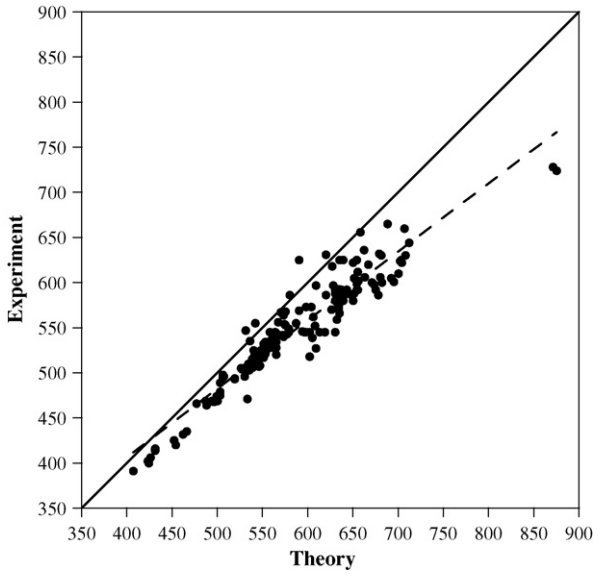

Fig. 3. Comparison between raw theoretical, and experimental λ_{max} for DA listed in Table 1. All values are in nm. The central line indicates a perfect theory/experiment match. The dashed lined corresponding to the linear fitting of Eq. (1).

A graphical comparison between theoretical and experimental λ_{max} is plotted in Fig. 3. As expected [57], theory tends to moderately overestimate the absorption wavelength, with only 5 out of 185 cases showing theoretical underestimation. The computed mean signed error (MSE, experiment-theory) is −39 nm, or 0.14 eV. The corresponding absolute deviation (MAE) reaches 40 nm, or 0.15 eV. Note that the average deviations are not significantly structure-dependent, as the MAE for the series **I** (**X**) is 0.16 eV (0.14 eV). These MAE stand in between the deviations noted for cyclopentene-DA (74 nm) [56] and maleic DA (9 nm) [54]. In any case, the 0.15 eV average error is perfectly in the line of the expected PCM-TD-PBE0 accuracy determined for a very extended set of organic dyes [57] or for Rydberg states using the same functional [79]. Note that usually, the typical TD-DFT/experiment discrepancies tend to be significantly larger, i.e. 0.2–0.3 eV, especially when small basis sets and gas-phase models are used [80–83]. It is obvious from Fig. 3 and from the overestimated auxochromic shifts (see above) that the TD-DFT errors tend to increase with the λ_{max}. However, a simple linear regression could correct the *ab* initio values. For the complete 185 cases, we obtain:

$$\lambda_{max}{}^{SLR} = 103.05 + 0.7585(4)\lambda_{max}{}^{TD\text{-}DFT} \quad (1)$$

$$E^{SLR} = 0.327(73) + 0.9138(2)E^{TD\text{-}DFT} \quad (2)$$

in the nm and eV scales, respectively. These equations provide R^2 of 0.90 and 0.93, respectively. The MAE after statistical corrections are 13 nm and 0.05 eV, respectively, that is about three times smaller than the uncorrected results. We can therefore state that our model delivers consistent evaluations of the auxochromic shifts, Eqs. (1) and (2) allowing quantitative agreement with experiment.

3.2. Further discussion

Before investigating structure–property relationships, we have studied the topology of the frontier orbitals for some typical complexes. Indeed, for all compounds, we have found that the transition responsible for the colour presents a strong HOMO-LUMO character, associated to a large oscillator force. The three most effective chemical modifications have been considered, that is (i) adding side groups, (ii) substituting heteroatoms, and (iii) varying the symmetry. The HOMO and LUMO of four DA from series **I** are depicted in Fig. 4. It turns out that the HOMO always have similar shapes, i.e. the occupied frontier orbital appears almost unaffected by the presence (or not) of side groups. Indeed, while all HOMO display strong contributions on the sulphur atoms and on the central double bonds, negligible densities are brought by aldehyde or phenyl moieties. This is in good agreement with the results obtained for maleic [49] and cyclopentene DA [56]. For the photoactive centre, the LUMO are located on the single bonds (see Fig. 1), i.e. electronic absorption leads to a modification of the double/single bond pattern, as usual in conjugated organic molecules. In addition, all LUMO show significant electron densities on the aldehyde or phenyl, i.e. the LUMO are more delocalized (and therefore stabilized) when the π path extends along the R_2 groups. Indeed, the decrease of the LUMO energy accounts for about 2/3 the electronic gap narrowing upon substitution. This correlates with the increase of λ_{max} noted upon the addition of electron withdrawing side groups. Additionally, the photon absorption for the three largest DA given Fig. 4 implies a significant electronic transfer from the centre of the molecule to its periphery: such phenomenon explains why TD-PBE0 error tends to increase for DA with small transition energies (see Section 3.1). Fig. 5 is a sketch of the topology of the HOMO and LUMO for DA from series **X**, with one of the five-member rings successively containing S, NMe, CH_2 or SO_2 groups. It is clear that the HOMO are much more sensitive than the LUMO to the modification of the heteroatom. Indeed, all LUMO display similar topologies, that are comparable to these of Fig. 4. Plugging a NMe group mostly localizes the HOMO on the right hand side of the molecule and increases its energy (same repulsion, smaller delocalization). On the contrary, using a SO_2-containing ring hinders the delocalization, that is, the density is mainly located on the non-oxidized part of the DA, leading to a stabilization of the HOMO as the initial repulsion between the two sulphur atoms is reduced. Therefore, for NMe- and SO_2-bearing photochroms, the modifications of the HOMO level prevail for colour variation. This latter conclusion is in perfect agreement with recent simulations of sulphur-oxidized DA [53]. In Fig. 6, the frontier orbitals have been plotted for structural DA isomers belonging to series **I**, **IV** and **II**. The HOMO of **II** is relatively similar to the HOMO of **I** (given the unlike symmetry), though the electron density on the thiophene double bonds is smaller than for **I**. This induces less repulsion between the two thiophene rings, and the HOMO of **II** is thus more stabilized than the one of **I**. On the contrary, the LUMO is strongly affected,as it is only localized on the perfluoro ring and the two side carbon atoms. In other words, the LUMO of **II** is consequently much more localized and of higher energy than **I**'s. As the HOMO (LUMO) in **II** is of lower (higher) energy than in **I**, the energy gap is also larger, and the λ_{max} smaller. For its part, **IV** offers an intermediate situation. These conclusions also back the thiazolyl-DA orbital plots found in Ref. [46].

Two recent studies on other DA derivatives [51,56] established a nice correlation between the bond length alternation (BLA) computed in the chromophoric unit, and the λ_{max}. The BLA, computed as the normalized difference between the lengths of the single and double bonds involved in the HOMO (see **I** of Fig. 1 for atom numbering) writes:

$$BLA = \frac{1}{3}(d_{2-3} + d_{2'-3'} + d_{4-4'}) - \frac{1}{4}(d_{1-2} + d_{1'-2'} + d_{3-4} + d_{3'-4'}) \quad (3)$$

and is often viewed as the geometrical parameter best describing π-electron mobility in delocalised systems, such as polymers or dyes [84–88]. A few crystal structures of closed-ring DA are available [89–93] and allow comparisons with our results. For **I** with X =S, R_1=H, R_2=Ph, and R_3=Me, we obtain a BLA of 0.065 Å in good agreement with the X-ray value of 0.063 Å [89]. Adding Me groups at R_1 increases the theoretical (0.081 Å) and experimental (0.078 Å)

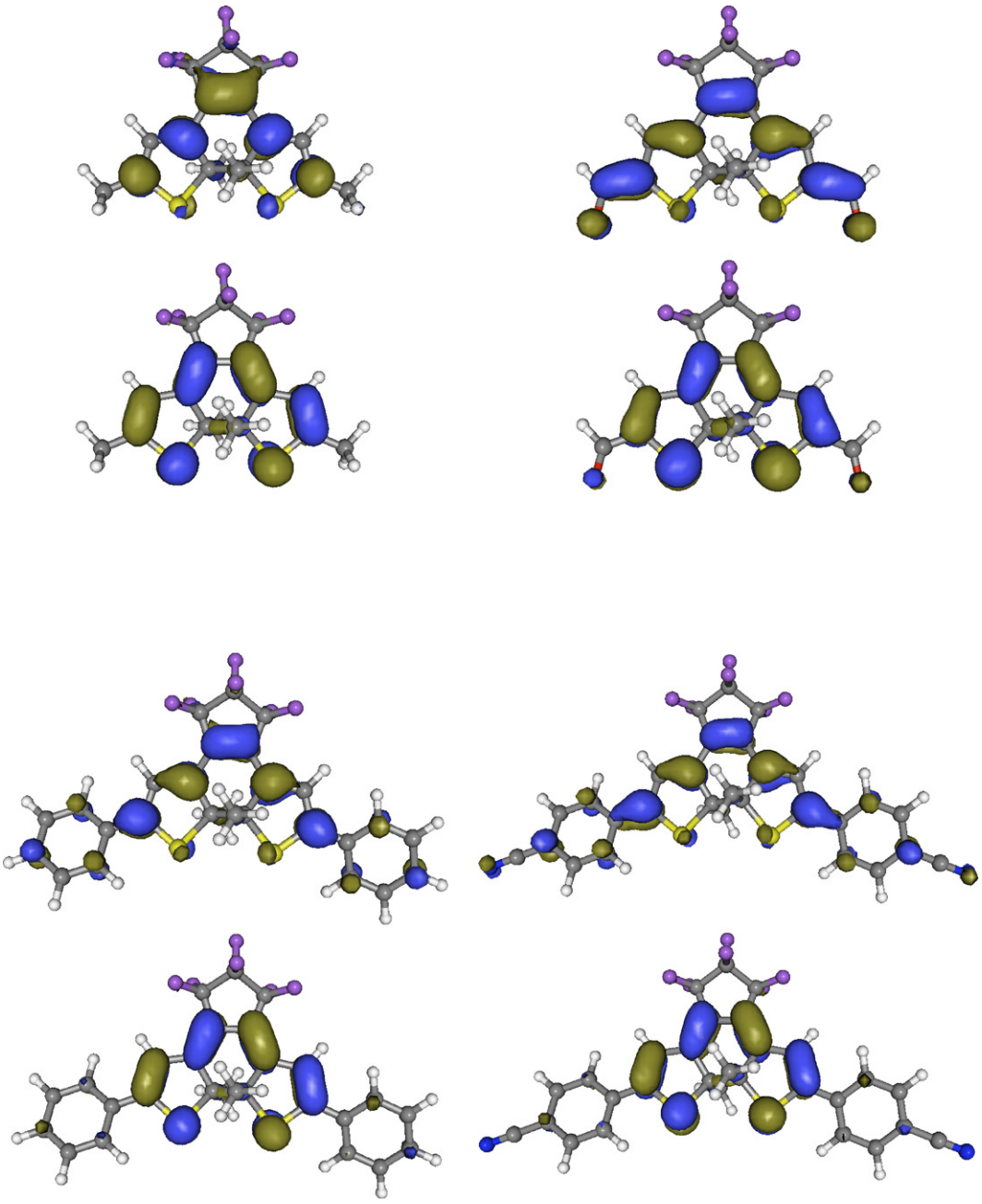

Fig. 4. Frontier orbitals (contour threshold of 0.04 a.u.) of **I** with Me (top left), CHO (top right), Ph (bottom left) and *p*-CN-Ph (bottom right) side groups. For each compound, the HOMO (LUMO) is located at the bottom (top).

values [93], whereas increasing the alkyl size leads the opposite trends in both methods [92]. For **X** (X=S) with two side nitro groups, two molecules per unit cell are found with BLA of 0.082 and 0.079 Å, whereas we obtain a smaller estimate (0.069 Å). For the full set of molecules belonging to series **I**, the PBE0 BLA varies from 0.099 Å to 0.045 Å, with most values being in between 0.055 Å and 0.085 Å. A similar variation range was found for cyclopentene-DA [56]. There is indeed a qualitative relationship between the BLA and the experimental λ_{max}, smaller BLA being associated to more equal single and double-bond lengths. In other words, the more delocalized systems present smaller excitation energies and larger λ_{max}. The linear correlation coefficient, *R*, for this purely empirical rule is weak however (0.76) and is far from being competitive with respect to the TD-DFT efficiency (*R*=0.90 for the same set of molecules). The situation is even worse when considering the set of molecules **X**-**XIII** that show similar structures. Indeed, as Eq. (3) does not take into account the more extended nature of the chromophoric unit that spans on the whole aromatic rings for **X** –**XIII** (see Fig. 5), the *R* falls to a ridiculous 0.32. This clearly indicates that the BLA computed by Eq. (3) becomes a meaningless descriptor of the λ_{max}, showing that previous conclusions obtained in more limited set of dyes [51,56] could not be extended straightforwardly. Of course, one could modify the BLA definition depending on the selected series, but such a procedure would be intellectually disappointing.

The stability of the closed-ring DA is also an issue, as thermally unstable compounds are practically useless [6]. To assess the thermal stability, one formally needs to determine the activation energy, that is optimizing the transition-state, relating the open and the closed-ring forms, which is a demanding task for an homolytic bond formation in large conjugated structures. For this reason, we

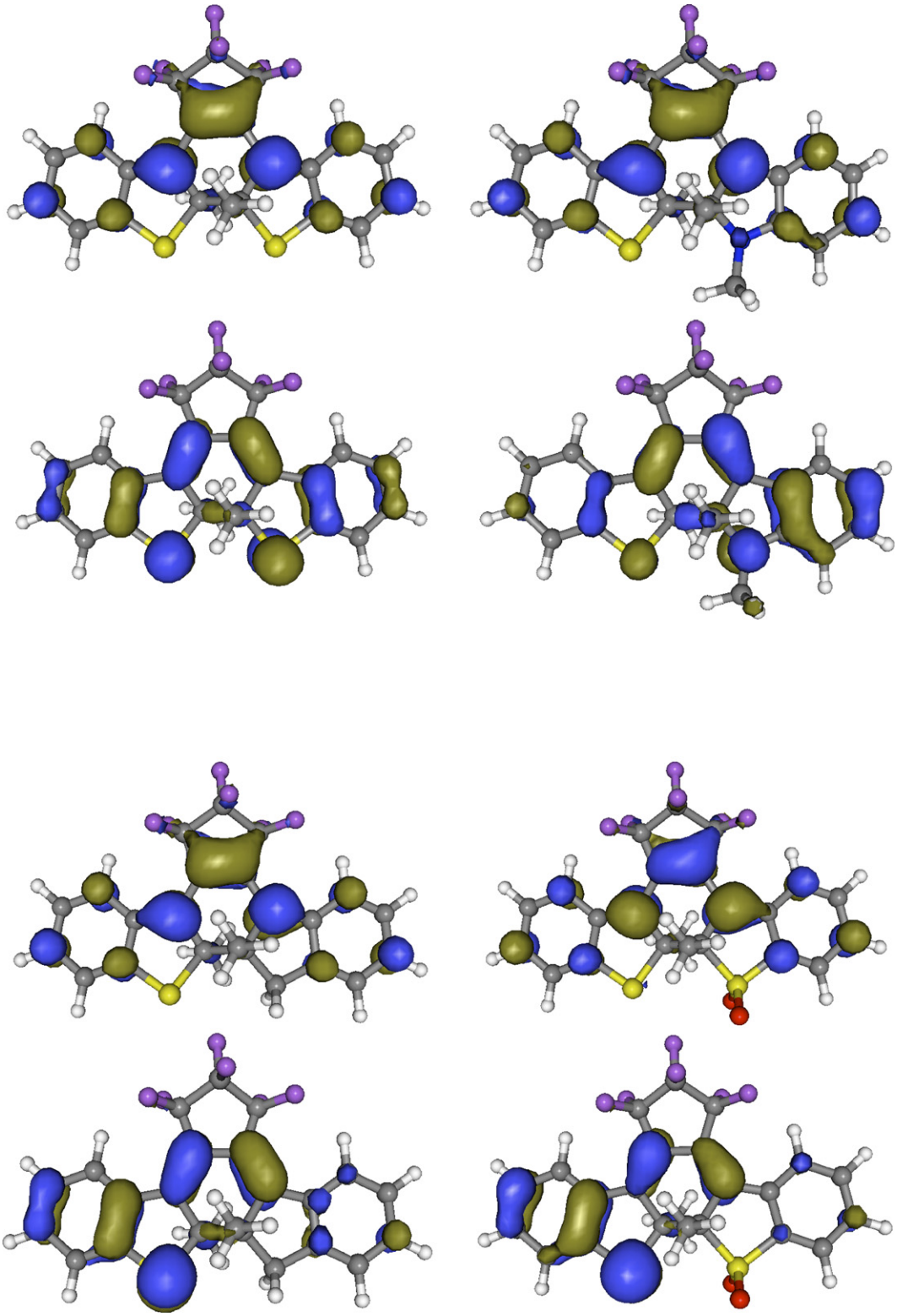

Fig. 5. PCM-TD-PBE0/6-311+G(2d,p) HOMO (bottom) and LUMO (top) of **X** with various heteroatoms: S, NMe, CH_2 and SO_2 (from top left to bottom right).

have established simple structure–stability relationships. First, we note that the Mulliken charges borne by the reactive carbon atoms are not an efficient indicator of the thermal stability. On the contrary, for a given series, the longer the central CC bond formed upon ring-closure, the least stable the DA. Indeed, for **I**, we got bond lengths smaller than 1.53 Å for X =S, $R_{1,3}$=Me, and R_2=Me or Ph, that are both stable for more than 12 h at 353 K [6], but bond lengths longer than 1.53 Å with aldehyde groups, with X =NMe, R_2=CN and with X = S and R_2=CH=C$(CN)_2$, these three latter systems having much smaller thermal half-time [6]. Note that such relationship is should be used carefully as the "threshold" bond length might vary when strongly modifying the nature of the DA,

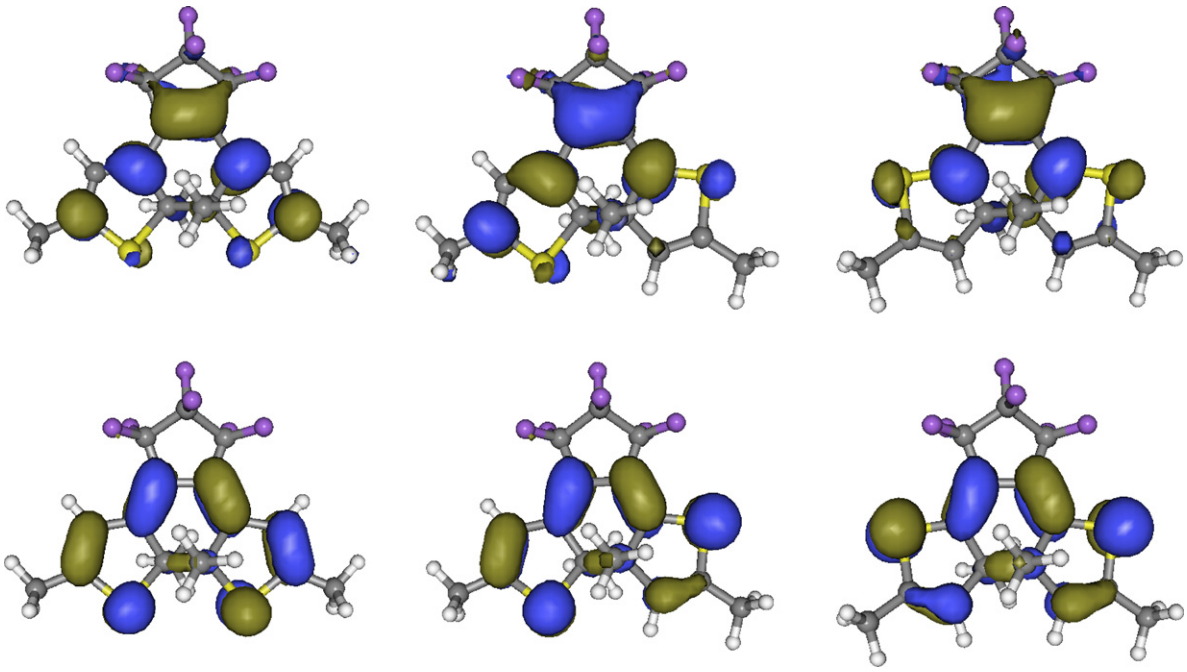

Fig. 6. HOMO (bottom) and LUMO (top) of **I** (left), **IV** (centre) and **II** (right) with methyl side groups. These plots have been obtained within the PCM-TD-PBE0/6-311+G(2d,p) level of theory using a contour threshold of 0.04 a.u.

and should therefore be conceptually replaced by more flexible limits.

4. Conclusions

Using a combination of the time-dependent density functional theory and the polarizable continuum model, we have investigated the visible absorption spectra of 185 perfluorocyclopentene diarylethenes. The theoretical approach, PCM-PBE0/6-311+G(2d,p)//PCM/6-311G(d,p) is able to simulate the effect of substitution, symmetry variations as well as heteroatom substitution, although problems pertain for alkoxy groups or solvatochromic effects. Using Eqs. (1) and (2), a quantitative theory/experiment agreement is achieved with MAE of 13 nm and 0.05 eV, respectively. The topology of the frontier orbitals can be correlated to the evolution of the λ_{max}. Indeed, adding side groups mostly modifies the LUMO, whereas changing the nature of the reactive rings implies stronger HOMO variations. For series **I**, the bond length alternation computed in the central part of the photochrom also relates to the λ_{max}. However, such a relationship does not hold for more delocalised DA such as type **X**. In addition, we have found that the ring–ring distance in the closed form can be qualitatively related to the experimental thermal stability within a given series of DA.

Acknowledgements

D.J. and E.A.P. thank the Belgian National Fund for Scientific Research for their research associate positions. The authors thank Prof. J.M. André and A. Laurent for their help. All calculations have been performed on the Interuniversity Scientific Computing Facility (ISCF), installed at the Facultés Universitaires Notre-Dame de la Paix (Namur, Belgium), for which the authors gratefully acknowledge the financial support of the FNRS-FRFC and the "Loterie Nationale" for the convention number 2.4578.02 and of the FUNDP.

References

[1] M. Irie, M. Mohri, J. Org. Chem. 53 (1988) 803.
[2] Y. Nakayama, K. Hayashi, M. Irie, J. Org. Chem. 55 (1990) 2592.
[3] S.L. Gilat, S.H. Kawai, J.M. Lehn, J. Chem. Soc., Chem. Commun. (1993) 1439.
[4] M. Irie, K. Sakemura, M. Okinaka, K. Uchida, J. Org. Chem. 60 (1995) 8305.
[5] S.L. Gilat, S.H. Kawai, J.M. Lehn, Chem. Eur. J. 1 (1995) 275.
[6] M. Irie, Chem. Rev. 100 (2000) 1685.
[7] B.L. Feringa, Molecular Switches, Wiley-VCH, Weinheim, 2001.
[8] M.M. Krayushkin, Chem. Heterocycl. Compd. 37 (2001) 15.
[9] H. Dürr, H. Bouas-Laurent, Photochromism Molecules and Systems, Elsevier, New York, 2003.
[10] K. Matsuda, M. Irie, J. Photochem. Photobiol. C: Photochem. Rev. 5 (2004) 169.
[11] H. Tian, S. Yang, Chem. Soc. Rev. 33 (2004) 85.
[12] K. Uchida, S. Nakamura, M. Irie, Bull. Chem. Soc. Jpn. 65 (1992) 430.
[13] M. Irie, K. Sayo, J. Phys. Chem. 96 (1992) 7671.
[14] M. Hanazawa, R. Sumiya, Y. Horikawa, M. Irie, J. Chem. Soc., Chem. Commun. (1992) 206.
[15] M.M. Krayushkin, V.A. Shirinyan, L.I. Belen'kii, A.A. Shimkin, A. Martynkin, B.M. Uzhinov, Russ. J. Org. Chem. 38 (2002) 1335.
[16] M.M. Krayushkin, S.N. Ivanov, A.Y. Martynkin, B.V. Lichitsky, A.A. Dudinov, B.M. Uzhinov, Russ. Chem. Bull. 50 (2001) 116.
[17] P.R. Hania, R. Telesca, L.N. Lucas, A. Pugzlys, J.H. van Esch, B.L. Feringa, J.G. Snijders, K. Duppen, J. Phys. Chem. A 106 (2002) 8498.
[18] L.N. Lucas, J.J. de Jong, J.H. van Esch, R.M. Kellogg, B.L. Feringa, Eur. J. Org. Chem. (2003) 155.
[19] Y. Chen, D.X. Zeng, M.G. Fan, Org. Lett. 5 (2003) 1435.
[20] M.M. Krayushkin, D.V. Pashchenko, B.V. Lichitskii, T.M. Valova, Y.P. Strokach, V.A. Barachevskii, Russ. J. Org. Chem. 42 (2006) 1816.
[21] Y. Chen, D.X. Zeng, N. Xie, Y.Z. Dang, J. Org. Chem. 70 (2005) 5001.
[22] Y. Han, Z.B. Zhang, J.P. Xiao, W.P. Yan, M.G. Fan, Chin. Chem. Lett. 16 (2005) 175.
[23] K. Matsuda, M. Irie, Chem. Eur. J. 7 (2001) 3466.
[24] G. Guirado, C. Coudret, J.-P. Launay, J. Phys. Chem. C 111 (2007) 2770.
[25] S. Kobatake, D. Takami, T. Muto, H. Ishikawa, M. Irie, Nature 446 (2007) 778.
[26] S. Nakamura, M. Irie, J. Org. Chem. 53 (1988) 6136.
[27] J. Ern, A.T. Benz, H.D. Martin, S. Mukamel, D. Schmid, S. Tretiaks, E. Tsiper, C. Kryschi, Chem. Phys. 246 (1999) 115.
[28] J. Ern, A.T. Benz, H.D. Martin, S. Mukamel, S. Tretiaks, K. Tsyganenko, K. Kuldova, H.P. Trommsdorff, C. Kryschi, J. Phys. Chem. A 105 (2001) 1741.
[29] D. Guillaumont, T. Kobayashi, K. Kanda, H. Miyasaka, K. Uchida, S. Kobatake, K. Shibata, S. Nakamura, M. Irie, J. Phys. Chem. A 106 (2002) 7222.
[30] K. Uchida, D. Guillaumont, E. Tsuchida, G. Mochizuki, M. Irie, A. Murakami, S. Nakamura, J. Mol. Struct. (THEOCHEM) 579 (2002) 115.
[31] Y. Asano, A. Murakami, T. Kobayashi, A. Goldberg, D. Guillaumont, S. Yabushita, M. Irie, S. Nakamura, J. Am. Chem. Soc. 126 (2004) 12112.
[32] Y. Liu, Q. Wang, Y. Liu, X.Z. Yang, Chem. Phys. Lett. 373 (2003) 338.

[33] Y. Asano, A. Murakami, T. Kobayashi, S. Kobatake, M. Irie, S. Yabushita, S. Nakamura, J. Mol. Struct. (THEOCHEM) 625 (2003) 227.
[34] A. Goldberg, A. Murakami, K. Kanda, T. Kobayashi, S. Nakamura, K. Ucjida, H. Sekiya, T. Fukaminato, T. Kawau, S. Kobatake, M. Irie, J. Phys. Chem. A 107 (2003) 4982.
[35] M. Cossi, V. Barone, J. Chem. Phys. 115 (2001) 4708.
[36] G. Scalmani, M.J. Frisch, B. Mennucci, J. Tomasi, R. Cammi, V. Barone, J. Chem. Phys. 124 (2006) 094107.
[37] M. Caricato, J. Mennucci, B. Tomasi, F. Ingrosso, R. Cammi, S. Corni, G. Scalmani, J. Chem. Phys. 124 (2006) 124520.
[38] D. Jacquemin, J. Preat, E.A. Perpète, Chem. Phys. Lett. 410 (2005) 254.
[39] D. Jacquemin, J. Preat, V. Wathelet, E.A. Perpète, J. Chem. Phys. 124 (2006) 074104.
[40] D. Jacquemin, J. Preat, V. Wathelet, M. Fontaine, E.A. Perpète, J. Am. Chem. Soc. 128 (2006) 2072.
[41] D.J. Tozer, J. Chem. Phys. 119 (2003) 12697.
[42] S. Yokojima, K. Matsuda, M. Irie, A. Murakami, T. Kobayashi, S. Nakamura, J. Phys. Chem. A 110 (2006) 8137.
[43] D. Jacquemin, E.A. Perpète, Chem. Phys. Lett. 429 (2006) 147.
[44] D. Majumdar, H.M. Lee, J. Kim, K.S. Kim, B.J. Mhin, J. Chem. Phys. 111 (1999) 5866.
[45] S. Kobatake, M. Morimoto, Y. Asano, A. Murakami, S. Nakamura, M. Irie, Chem. Lett. (2002) 1224.
[46] M. Giraud, A. Léaustic, M.F. Charlot, P. Yu, M. Césario, C. Philouze, R. Pansu, K. Nakatani, E. Ishow, New. J. Chem. 29 (2005) 439.
[47] K. Higashiguchi, K. Matsuda, A. Asano, A. Murakami, S. Nakamura, M. Irie, Eur. J. Org. Chem. (2005) 91.
[48] A.E. Clark, J. Phys. Chem. A 110 (2006) 3790.
[49] D.Z. Chen, Z. Wang, X. Zhao, J. Mol. Struct. (THEOCHEM) 774 (2006) 77.
[50] G. Guirado, C. Coudret, M. Hliwa, J.-P. Launay, J. Phys. Chem. B 109 (2005) 17445.
[51] A. Perrier, F. Maurel, J. Aubard, J. Photochem. Photobiol. A: Chem. 189 (2007) 167.
[52] A. Perrier, F. Maurel, J. Aubard, J. Phys. Chem. A 111 (2007) 9688.
[53] Y.C. Jeong, J.P. Han, Y. Kim, E. Kim, S.I. Yang, K.H. Ahn, Tetrahedron (2007) 3173.
[54] E.A. Perpète, D. Jacquemin, J. Photochem. Photobiol. A: Chem. 187 (2007) 40.
[55] A.M. Laurent, J.M. André, E.A. Perpète, D. Jacquemin, J. Photochem. Photobiol. A: Chem. 192 (2007) 211.
[56] E.A. Perpète, F. Maurel, D. Jacquemin, J. Phys. Chem. A 111 (2007) 5528.
[57] D. Jacquemin, E.A. Perpète, G.E. Scuseria, I. Ciofini, C. Adamo, J. Chem. Theory Comput. 4 (2008) 123.
[58] T. Yanai, D.P. Tew, N.C. Handy, Chem. Phys. Lett. 393 (2004) 51.
[59] M.J. Frisch, G.W. Trucks, H.B. Schlegel, G.E. Scuseria, M.A. Robb, J.R. Cheeseman, J.A. Montgomery, T. Vreven, K.N. Kudin, J.C. Burant, J.M. Millam, S.S. Iyengar, J. Tomasi, V. Barone, B. Mennucci, M. Cossi, G. Scalmani, N. Rega, G.A. Petersson, H. Nakatsuji, M. Hada, M. Ehara, K. Toyota, R. Fukuda, J. Hasegawa, M. Ishida, T. Nakajima, Y. Honda, O. Kitao, H. Nakai, M. Klene, X. Li, J.E. Knox, H.P. Hratchian, J.B. Cross, V. Bakken, C. Adamo, J. Jaramillo, R. Gomperts, R.E. Stratmann, O. Yazyev, A.J. Austin, R. Cammi, C. Pomelli, J.W. Ochterski, P.Y. Ayala, K. Morokuma, G.A. Voth, P. Salvador, J.J. Dannenberg, V.G. Zakrzewski, S. Dapprich, A.D. Daniels, M.C. Strain, O. Farkas, D.K. Malick, A.D. Rabuck, K. Raghavachari, J.B. Foresman, J.V. Ortiz, Q. Cui, A.G. Baboul, S. Clifford, J. Cioslowski, B.B. Stefanov, G. Liu, A. Liashenko, P. Piskorz, I. Komaromi, R.L. Martin, D.J. Fox, T. Keith, M.A. Al-Laham, C.Y. Peng, A. Nanayakkara, M. Challacombe, P.M.W. Gill, B. Johnson, W. Chen, M.W. Wong, C. Gonzalez, J.A. Pople Jr., Gaussian 03, Revision C.02 2004, Gaussian Inc., Wallingford, CT, 2004.
[60] C. Adamo, V. Barone, J. Chem. Phys. 110 (1999) 6158.
[61] M. Ernzerhof, G.E. Scuseria, J. Chem. Phys. 110 (1999) 5029.
[62] J.P. Perdew, K. Burke, M. Ernzerhof, Phys. Rev. Lett. 77 (1996) 3865.
[63] J.-F. Guillemoles, V. Barone, L. Joubert, C. Adamo, J. Phys. Chem. A 106 (2002) 11354.
[64] L. Petit, C. Adamo, N. Russo, J. Phys. Chem. B 109 (2005) 12214.
[65] A.D. Quartarolo, N. Russo, E. Sicilia, Chem. Eur. J. 12 (2006) 6797.
[66] D. Jacquemin, M. Bouhy, E.A. Perpète, J. Chem. Phys. 124 (2006) 204321.
[67] A. Pezzella, L. Panzella, O. Crescenzi, A. Napolitano, S. Navaratman, R. Edge, E. Land, V. Barone, M. d'Ischia, J. Am. Chem. Soc. 128 (2006) 15490.
[68] J. Tomasi, B. Mennucci, R. Cammi, Chem. Rev. 105 (2005) 2999.
[69] C.A. Bertolino, A.M. Ferrari, C. Barolo, G. Viscardi, G. Caputo, S. Coluccia, Chem. Phys. 330 (2006) 52.
[70] Heptane, for which the standard parameters have been defined in Gaussian03, has been used instead of hexane for these calculations.
[71] Heptane, for which the standard parameters have been defined in Gaussian03, has been used instead of 3-methyl-pentane for these calculations.
[72] For diethyl-ether, we have used: EPSINF = 1.828.
[73] Ethyl acetate, as diethylether except for: EPS = 6.02, EPSINF = 1.89 which have been set following available physico-chemical data.
[74] Note that vibrational, analysis has been performed for each molecule in a single solvent, but not in all solvents in order to gain cpu-time.
[75] C. Adamo, G.E. Scuseria, V. Barone, J. Chem. Phys. 111 (1999) 2889.
[76] L.A. Curtiss, K. Raghavachari, P.C. Referm, J.A. Pople, Chem. Phys. Lett. 270 (1997) 419.
[77] V. Barone, C. Adamo, J. Chem. Phys. 105 (1996) 11007.
[78] A. Peters, R. McDonald, N.R. Branda, Chem. Commun. (2002) 2274.
[79] I. Ciofini, C. Adamo, J. Phys. Chem. A 111 (2007) 5549.
[80] K. Burke, J. Werschnik, E.K.U. Gross, J. Chem. Phys. 123 (2005) 062206.
[81] D. Guillaumont, S. Nakamura, Dyes Pigments 46 (2000) 85.
[82] J. Fabian, Theor. Chem. Acc. 106 (2001) 199.
[83] J. Fabian, L.A. Diaz, G. Seifert, T. Niehaus, J. Mol. Struct. (THEOCHEM) 594 (2002) 41.
[84] J.L. Brédas, Adv. Mater. 7 (1995) 263.
[85] C.H. Choi, M. Kertesz, A. Karpfen, J. Chem. Phys. 107 (1997) 6712.
[86] R. Pino, G. Scuseria, J. Chem. Phys. 121 (2004) 8113.
[87] D. Jacquemin, E.A. Perpète, I. Ciofini, C. Adamo, Chem. Phys. Lett. 405 (2005) 376.
[88] D. Jacquemin, A. Femenias, H. Chermette, I. Ciofini, C. Adamo, J.M. André, E.A. Perpète, J. Phys. Chem. A 110 (2006) 5952.
[89] M. Irie, T. Lifka, S. Kobatake, N. Kato, J. Am. Chem. Soc. 122 (2000) 4871.
[90] S. Kobatake, M. Yamada, T. Yamada, M. Irie, J. Am. Chem. Soc. 121 (1999) 8450.
[91] T. Yamada, S. Kobatake, K. Muto, M. Irie, J. Am. Chem. Soc. 122 (2000) 1589.
[92] S. Kobatake, K. Shibata, K. Uchida, M. Irie, J. Am. Chem. Soc. 122 (2000) 12135.
[93] M. Irie, S. Kobatake, M. Horichi, Science 291 (2001) 1769.
[94] M. Takeshita, M. Ogawa, K. Miyata, T. Tamato, J. Phys. Org. Chem. 16 (2003) 148.
[95] M. Irie, K. Uchida, T. Eriguchi, H. Tsuzuki, Chem. Lett. (1995) 899.
[96] K. Uchida, M. Irie, Chem. Lett. (1995) 969.
[97] M. Irie, T. Eriguchi, T. Takada, K. Uchida, Tetrahedron 53 (1997) 1263.
[98] S. Kobatake, M. Irie, Tetrahedron 59 (2003) 8359.
[99] K. Uchida, T. Matsuoka, K. Sayo, M. Iwamoto, S. Hayashi, M. Irie, Chem. Lett. (1999) 835.
[100] A. Heynderickx, A.M. Kaou, C. Moustrou, A. Samat, R. Guglielmetti, New. J. Chem. 27 (2003) 1425.
[101] H. Miyasaka, T. Nobuto, A. Itaya, N. Tamai, M. Irie, Chem. Phys. Lett. 269 (1997) 281.
[102] L.N. Lucas, PhD Thesis, Rijksuniversiteit Groningen, Groningen, Netherlands, 2001.
[103] W.R. Browne, J.J. deJong, T. Kudernac, M. Walko, L.N. Lucas, K. Uchida, J.H. van Esch, B.L. Feringa, Chem. Eur. J. 11 (2005) 6430.
[104] Y.P. Strokach, T.M. Valova, Z.O. Golotyuk, V.A. Barachevsky, V.N. Yarovenko, M.A. Kalik, M.M. Krayushkin, Opt. Spectrosc. 99 (2005) 714.
[105] M. Morimoto, M. Irie, Chem. Eur. J. 12 (2006) 4275.
[106] V.A. Barachevsky, Y.P. Strokach, M.M. Krayushkin, Mol. Cryst. Liq. Cryst. 430 (2005) 181.
[107] M.M. Krayushkin, M.A. Kalik, D.L. Dzhavadov, A.Y. Martynkin, A.V. Firsov, B.M. Uzhinov, Russ. Chem. Bull. 48 (1999) 971.
[108] M.M. Krayushkin, M.A. Kalik, D.L. Dzhavadov, L.G. Vorontsova, Z.A. Starikova, A.Y. Martynkin, S.N. Ivanov, B.M. Uzhinov, Russ. Chem. Bull. 49 (2000) 1757.
[109] S. Pu, F.S. Zhang, F. Sun, R.J. Wang, X.H. Zhou, S.K. Chan, Tetrahedron Lett. 44 (2004) 1011.
[110] M. DelZoppo, A. Lucotti, G. Zerbi, Vib. Spectrosc. 43 (2007) 249.
[111] N. Tamai, T. Saika, T. Shimidzu, M. Irie, J. Phys. Chem. 100 (1996) 4689.
[112] K. Uchida, N. Izumi, S. Sukata, Y. Kojima, S. Nakamura, M. Irie, Angew. Chem. Int. Ed. Engl. 45 (2006) 6470.
[113] S. Pu, J. Xu, L. Shen, Q. Xiao, T. Yang, G. Li, Tetrahedron Lett. 46 (2005) 871.
[114] S. Pu, T. Yang, Y. Wang, F. Zhang, J. Xu, Spectrochim. Acta A 66 (2007) 335.
[115] A. Peters, N.R. Branda, Chem. Commun. (2003) 954.
[116] M. Morimoto, S. Kobatake, M. Irie, Mol. Cryst. Liq. Cryst. 431 (2005) 151.
[117] M. Murakami, H. Miyasaka, T. Okada, S. Kobatake, M. Irie, J. Am. Chem. Soc. 126 (2004) 14764.
[118] P.R. Hania, A. Pugzlys, L.N. Lucas, J.J.D. deJong, B.L. Feringa, J.H. van Esch, H.T. Jonkman, K. Duppen, J. Phys. Chem. A 109 (2005) 9437.
[119] W.R. Browne, J.J. deJong, T. Kudernac, M. Walko, L.N. Lucas, K. Uchida, J.H. van Esch, B.L. Feringa, Chem. Eur. J. 11 (2005) 6414.
[120] S. Kobatake, K. Uchida, E. Tsuchida, M. Irie, Chem. Lett. (2000) 1340.
[121] K. Morimitsu, K. Shibata, S. Kobatake, M. Irie, J. Org. Chem. 67 (2002) 4574.
[122] S. Yamamoto, K. Matsuda, M. Irie, Chem. Eur. J. 9 (2003) 4878.
[123] S. Yamamoto, K. Matsuda, M. Irie, Angew. Chem. Int. Ed. 42 (2003) 1636.
[124] S. Pu, T. Yang, G. Li, J. Xu, B. Chen, Tetrahedron Lett. 47 (2006) 3167.
[125] S. Pu, T. Yang, B. Yao, Y. Wang, M. Lei, J. Xu, Mater. Lett. 61 (2007) 855.
[126] S. Pu, Q. Xiao, J.K. Xu, L. Shen, G.Z. Li, B. Chen, Chin. J. Chem. 24 (2006) 463.
[127] S. Pu, T. Yang, J. Xu, L. Shen, G. Li, Q. Xiao, B. Chen, Tetrahedron 61 (2005) 6623.
[128] S.H. Kawai, S.L. Gilat, J.M. Lehn, J. Chem. Soc., Chem. Commun. (1994) 1011.
[129] S.H. Kawai, S.L. Gilat, R. Ponsinet, J.M. Lehn, Chem. Eur. J. 1 (1995) 285.
[130] J. Biteau, F. Chaput, K. Lahlil, J.P. Boilot, G.M. Tsivgoulis, J.M. Lehn, B. Darracq, C. Marois, Y. Lévy, Chem. Mater. 10 (1945) 19998.
[131] M. Morimoto, S. Kobatake, M. Irie, Chem. Eur. J. 9 (2003) 621.
[132] X.D. Liu, Z.H. Chen, G.F. Fan, F.S. Zhang, Chin. J. Chem. 24 (2006) 1462.
[133] S. Iwata, Y. Ishihara, C.P. Qian, I. Tanaka, J. Org. Chem. 57 (1992) 3726.
[134] K. Uchida, T. Ishikawa, M. Takeshita, M. Irie, Tetrahedron 54 (1998) 6627.
[135] K. Higashiguchi, K. Matsuda, M. Matsuo, T. Yamada, M. Irie, J. Photochem. Photobiol. A. 152 (2002) 141.
[136] T. Fukaminato, T. Kawai, S. Kobatake, M. Irie, J. Phys. Chem. B 107 (2003) 8372.
[137] S. Takami, T. Kawai, M. Irie, Eur. J. Org. chem. (2002) 3796.
[138] F. Sun, F. Zhang, H. Guo, X. Zhou, R. Wang, F. Zhao, Tetrahedron 59 (2003) 7615.
[139] S. Takami, M. Irie, Tetrahedron 60 (2004) 6155.
[140] S. Pu, T. Yang, J. Xu, B. Chen, Tetrahedron Lett. 47 (2006) 6473.
[141] T. Yamaguchi, Y. Fujita, M. Irie, Chem. Commun. (2004) 1010.
[142] M. Irie, K. Uchida, Bull. Chem. Soc. Jpn. 71 (1998) 985.
[143] T. Yamaguchi, M. Irie, Tetrahedron Lett. 47 (2006) 1267.
[144] K. Uchida, S. Nakamura, M. Irie, Res. Chem. Intermediat. 21 (1995) 861.
[145] K. Yagi, M. Irie, Bull. Chem. Soc. Jpn. 76 (2003) 1625.

[146] T. Yamaguchi, M. Irie, J. Org. Chem. 70 (2005) 10323.
[147] T. Yamaguchi, M. Irie, Bull. Chem. Soc. Jpn. 79 (2006) 1100.
[148] K. Uchida, E. Tsuchida, Y. Aoi, S. Nakamura, M. Irie, Chem. Lett. (1999) 63.
[149] M. Frigoli, G.H. Mehl, Chem. Commun. (2004) 818.
[150] E. Kim, M. Kim, K. Kim, Tetrahedron 62 (2006) 6814.
[151] K. Matsuda, M. Irie, Tetrahedron Lett. 41 (2000) 2577.
[152] T. Yamaguchi, Y. Fujita, H. Nakazumi, S. Kobatake, M. Irie, Tetrahedron 60 (2004) 9863.
[153] N. Taifuji, K. Matsuda, M. Irie, Org. Lett. 7 (2005) 3777.
[154] T. Yamaguchi, M. Irie, J. Photochem. Photobiol. A 178 (2006) 162.
[155] Y.C. Jeong, D.G. Park, E. Kim, K.H. Ahn, S.I. Yang, Chem. Commun. (2006) 1881.
[156] Y.C. Jeong, S.I. Yang, K.H. Ahn, E. Kim, Chem. Commun. (2005) 2503.